

SCIENTIFIC REPORTS

OPEN

Nb₂O₅- γ -Al₂O₃ nanofibers as heterogeneous catalysts for efficient conversion of glucose to 5-hydroxymethylfurfural

Received: 21 April 2016
Accepted: 06 September 2016
Published: 26 September 2016

Huanfeng Jiao¹, Xiaoliang Zhao¹, Chunxiao Lv¹, Yijun Wang¹, Dongjiang Yang^{1,2}, Zhenhuan Li³ & Xiangdong Yao^{1,2}

One-dimensional γ -Al₂O₃ nanofibers were modified with Nb₂O₅ to be used as an efficient heterogeneous catalyst to catalyze biomass into 5-hydroxymethylfurfural (5-HMF). At low Nb₂O₅ loading, the niobia species were well dispersed on γ -Al₂O₃ nanofiber through Nb–O–Al bridge bonds. The interaction between Nb₂O₅ precursor and γ -Al₂O₃ nanofiber results in the niobia species with strong Lewis acid sites and intensive Brønsted acid sites, which made 5-HMF yield from glucose to reach the maximum 55.9–59.0% over Nb₂O₅- γ -Al₂O₃ nanofiber with a loading of 0.5–1 wt% Nb₂O₅ at 150 °C for 4 h in dimethyl sulfoxide. However, increasing Nb₂O₅ loading could lead to the formation of two-dimensional polymerized niobia species, three-dimensional polymerized niobia species and crystallization, which significantly influenced the distribution and quantity of the Lewis acid sites and Brønsted acid sites over Nb₂O₅- γ -Al₂O₃ nanofiber. Lewis acid site Nb^{δ+} played a key role on the isomerization of glucose to fructose, while Brønsted acid sites are more active for the dehydration of generated fructose to 5-HMF. In addition, the heterogeneous Nb₂O₅- γ -Al₂O₃ nanofiber catalyst with suitable ratio of Lewis acid to Brønsted sites should display an more excellent catalytic performance in the conversion of glucose to 5-HMF.

Fossil-based resources such as petroleum, coal and natural gas are deemed as the dominant raw materials to be used for energy and synthesis of organic chemicals^{1,2}. Nevertheless, the mismatch between the increasing demand for and sharply diminishing supply of fossil-based resources implies that the search for alternative raw material sources is critically important. Renewable biomass is the most suitable candidate for alternative raw material sources since they are abundant, easy to obtain and rich of carbohydrates which can be converted to valuable chemicals^{3,4}. Consequently, the conversion of renewable biomass to fuels and chemicals has received wide attention.

Cellulose as an important branch of biomass is composed of the basic glucose unit building blocks that can be transformed to the useful platform molecule 5-HMF. 5-HMF can act as the raw material to be used to synthesize chemicals, liquid fuels and so on ref. 5 and 6. Hence, developing an approach to efficiently synthesize 5-HMF from rich and cheap glucose resources under mild conditions is extremely desirable.

5-HMF synthesis from glucose is difficult due to the high stability of the glucose ring, making the dehydration process more difficult⁷. In order to overcome this disadvantage, the catalysts were paid more attention to reduce the activation energy of this reaction. Catalysts used for glucose dehydration to 5-HMF are classified into heterogeneous and homogeneous catalysts which play the different performance in different reaction solvents such as aqueous, organic solvents and ionic liquids^{8,9}. Homogeneous catalysts like ionic liquids and metal salts employed for 5-HMF conversion from glucose are limited due to several drawbacks including the high cost, toxicity, difficult separation and recovery^{10,11}. In contrast, heterogeneous catalysts avoided aforementioned disadvantage

¹Collaborative Innovation Center for Marine Biomass Fibers, Materials and Textiles of Shandong Province; College of Chemistry, Chemical and Environmental Engineering, Qingdao University, Qingdao 266071, China. ²Queensland Micro- and Nanotechnology Centre (QMNC), Griffith University, Nathan, Brisbane, QLD 4111, Australia. ³State Key Laboratory of Separation Membranes and Membrane Processes, School of Materials Science and Engineering, Tianjin Polytechnic University, 300160 Tianjin, China. Correspondence and requests for materials should be addressed to D.Y. (email: yjd0203@gmail.com) or Z.L. (email: lizhenhuan@tjpu.edu.cn) or X.Y. (email: x.yao@griffith.edu.au)

Catalyst	Nb ⁵⁺ concentration (mg/L)	Nb ₂ O ₅ content controlled (wt%)	Nb ₂ O ₅ real content (wt%)
1 wt% Nb ₂ O ₅ -Al ₂ O ₃	0.046	1	1.0
3 wt% Nb ₂ O ₅ -Al ₂ O ₃	0.014	3	3.0
5 wt% Nb ₂ O ₅ -Al ₂ O ₃	0.016	5	3.4
10 wt% Nb ₂ O ₅ -Al ₂ O ₃	0.022	10	4.7
15 wt% Nb ₂ O ₅ -Al ₂ O ₃	0.044	15	9.4
30 wt% Nb ₂ O ₅ -Al ₂ O ₃	0.124	30	26.6
40 wt% Nb ₂ O ₅ -Al ₂ O ₃	0.158	40	33.9

Table 1. The Nb₂O₅ contents of Nb₂O₅- γ -Al₂O₃ by ICP-AES.

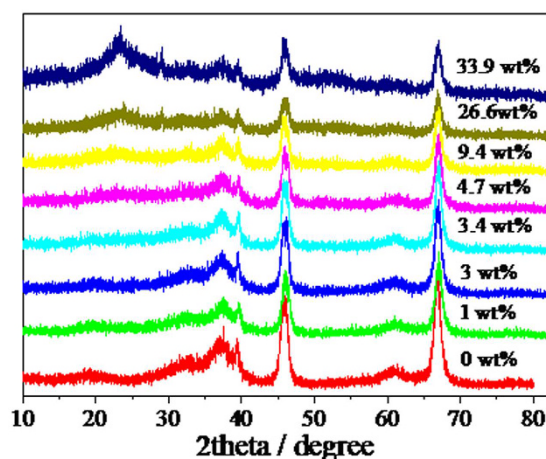


Figure 1. XRD of γ -Al₂O₃ with different Nb₂O₅ loadings.

have been widely utilized for biomass conversion into 5-HMF, e.g. oxides, phosphates, ion exchange resins and heteropolyacids^{12,13}.

As for the heterogeneous catalysts, besides the main catalytic active sites like metal oxides such as WO₃, TiO₂, and ZrO₂, the supports also play a very important role on catalytic process^{14,15}. Generally, the conventional porous materials were used as supports because of their large surface areas. But the porosity and surface area will be reduced during the loading of active sites. Recently, various one-dimensional (1D) oxide nanofibers have been reported as the efficient heterogeneous catalyst supports, which can realize the loading of active sites without declining surface area^{16,17}.

Herein, the active sites (acidic Nb₂O₅) were loaded on the surface of 1D γ -Al₂O₃ nanofibers by facile incipient-wetness impregnation method. Nb₂O₅- γ -Al₂O₃ nanofibers displayed the high catalytic activity in glucose conversion to 5-HMF with dimethyl sulfoxide as solvent, and it was found that Lewis acid site Nb^{δ+} promoted the isomerization of glucose to fructose, while Brønsted acid sites catalyzed the dehydration of generated fructose to 5-HMF.

Results and Discussion

Nb₂O₅/ γ -Al₂O₃ nanofiber characterization. 1D γ -Al₂O₃ nanofiber with different Nb₂O₅ loading of 0, 1, 3, 3.4, 4.7, 9.4, 26.6 and 33.9 wt% was prepared by facile incipient-wetness impregnation method. Table 1 presents the contents of Nb₂O₅ measured by ICP-AES technique (after the samples were dissolved by strong phosphoric acid). The characterized results reveal that the actual Nb₂O₅ contents are same or smaller than the controlled Nb₂O₅ content.

XRD patterns were collected from 5 to 80° (Fig. 1). It is found that the distinct diffraction peaks of these samples appear at 37.6°, 39.5°, 45.8°, 60.9° and 67°, which are assigned to the diffraction of (3 1 1), (2 2 2), (4 0 0), (5 1 1) and (4 4 0) of γ -Al₂O₃, respectively. With the increase of Nb₂O₅ loading, the intensive diffraction peaks at $2\theta = 22.6^\circ$ and 28.5° appeared, which are assigned to the diffraction of bulk Nb₂O₅¹⁸.

Textural properties of catalysts obtained from the nitrogen sorption at 77 K are listed in Table 2 and Fig. 2. These isotherms are similar with each other which belong to the type IV Van Der Waals isotherm¹⁹. Both pore volume and average pore diameters decrease with the increase of Nb₂O₅ loading, but the BET surface areas of Nb₂O₅- γ -Al₂O₃ nanofibers gradually increase with Nb₂O₅ loading augment. However, further increasing Nb₂O₅ loading will lead to BET surface area decrease, which is similar with the report of literature²⁰.

The scan electron microscopy (SEM) images of γ -Al₂O₃ nanofiber with different Nb₂O₅ loading from 0 to 33.9 wt% are presented in Fig. 3a–h. All samples have the homogeneous length of 200–300 nm and the similar

Sample (wt%)	BET surface ($\text{m}^2 \text{g}^{-1}$)	Pore volume ($\text{cm}^3 \text{g}^{-1}$)	Average pore diameter (nm)	
			BJH adsorption	BJH desorption
0	70.86	0.63	26.93	26.42
1	74.02	0.61	27.79	25.39
3	73.36	0.55	25.30	24.92
3.4	81.75	0.48	22.86	23.70
4.7	116.49	0.46	17.21	21.88
9.4	130.99	0.32	10.77	14.29
26.6	123.18	0.25	1.45	1.85
33.9	103.63	0.23	1.40	1.90

Table 2. The textural properties of $\gamma\text{-Al}_2\text{O}_3$ with different Nb_2O_5 loadings.

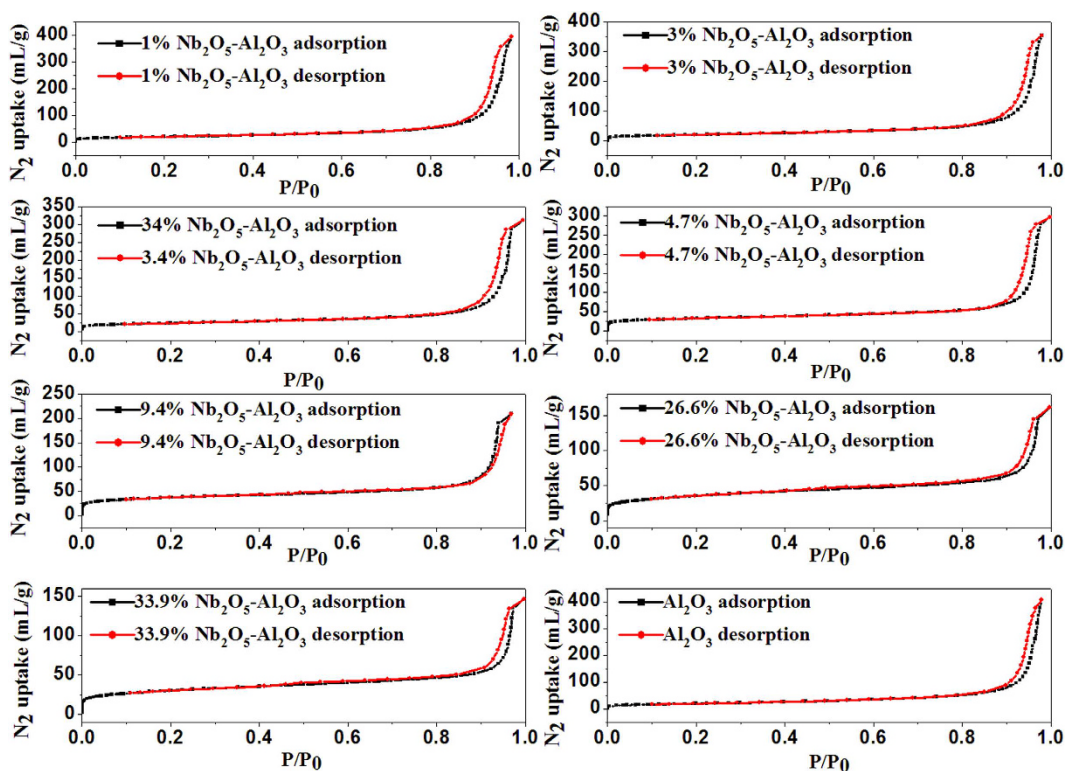


Figure 2. The N_2 sorption isotherms at 77 K for $\gamma\text{-Al}_2\text{O}_3$ (solid circles: adsorption; open circles: desorption).

diameter of 30–50 nm, which indicates Nb_2O_5 loading do not influence the morphology and structure of $\gamma\text{-Al}_2\text{O}_3$ nanofibers. However, the particles are observed to aggregate together when Nb_2O_5 loading reaches 4.7 wt%, due to the surface tension^{21,22}. Moreover, the characterization of $\gamma\text{-Al}_2\text{O}_3$ and 1 wt% $\text{Nb}_2\text{O}_5\text{-}\gamma\text{-Al}_2\text{O}_3$ by transmission electron microscopy (TEM) was also performed. As shown in Fig. 4a,b, the average size and the morphology of these particles are similar. Elemental mapping by EDS was used to study the distribution of the Al, O, and Nb elements in nanofiber based samples (Fig. 4d). The abundant Al and O elements distribute homogeneously in a single nanofiber, however the content of Nb element is comparably smaller and Nb element mainly distributes on the surface of $\gamma\text{-Al}_2\text{O}_3$.

As shown in Fig. 5, $\gamma\text{-Al}_2\text{O}_3$ nanofiber exhibits the very weak Raman bands in the region of 200–2000 cm^{-1} due to the low polarizability of light atoms and the ionic character of Al–O bonds²³. As for $\text{Nb}_2\text{O}_5\text{-}\gamma\text{-Al}_2\text{O}_3$ nanofiber with 1–9.4 wt % load, the intensive Raman bands in the region of 1000–2000 cm^{-1} appeared due to the polarizability of Nb–O–Al species²⁴.

Effects of different Nb_2O_5 loading on biomass selectivity conversion. Under the condition of 150 °C for 4 hours, 5-HMF yield from glucose is in the range of 32.5% to 59.0% with the different Nb_2O_5 loading (Fig. 6A), and the best 5-HMF yield is about 59.0% over the catalyst with 0.5 wt% Nb_2O_5 loading, while the yield is only 33.5% with 33.9 wt% Nb_2O_5 loading. 59.0% 5-HMF yield over 0.5 wt% $\text{Nb}_2\text{O}_5\text{-}\gamma\text{-Al}_2\text{O}_3$ nanofiber is significant which is higher than those reported in literatures^{20,25,26}. $\text{Nb}_2\text{O}_5\text{-}\gamma\text{-Al}_2\text{O}_3$ nanofiber can well catalyze

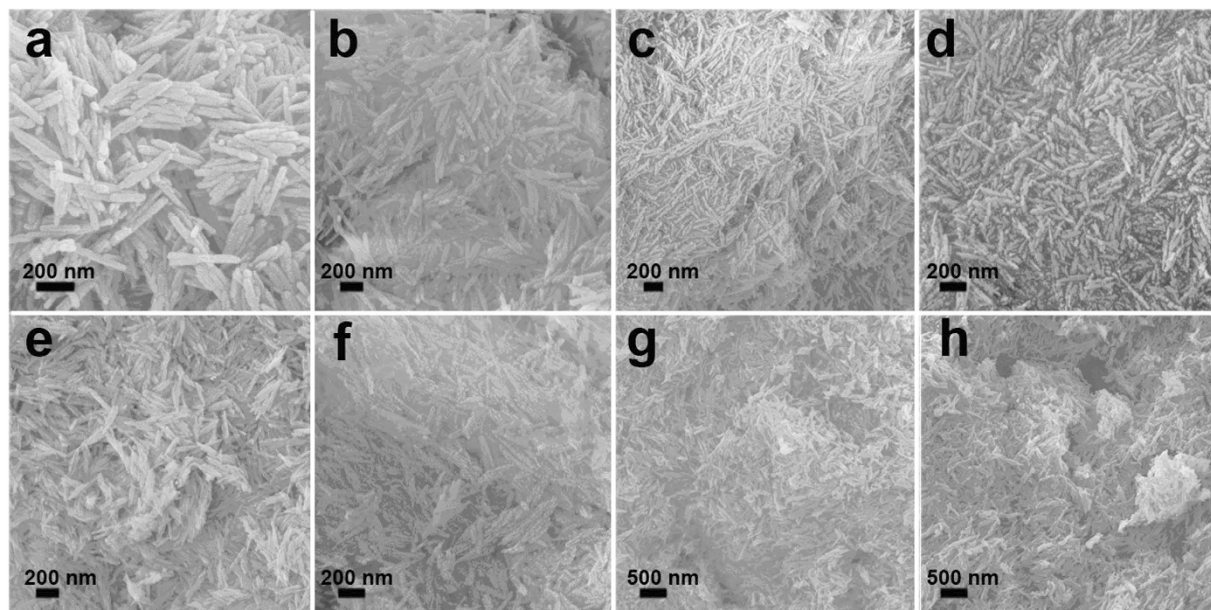


Figure 3. SEM images of γ - Al_2O_3 with different Nb_2O_5 loadings: (a) 0 wt%; (b) 1 wt%; (c) 3 wt%; (d) 3.4 wt%; (e) 4.7 wt%; (f) 9.4 wt%; (g) 26.6 wt%; (h) 33.9 wt%.

the conversion of fructose and xylose to 5-HMF and furfural, which is not as significant as glucose conversion (Fig. 6B,C). As Nb_2O_5 loading increased from 3 wt% to 33.9 wt%, 5-HMF yields from fructose conversion raised from 67.4% to 76.8%, but 3 wt% Nb_2O_5 loading resulted in the minimum 5-HMF yield. When xylose was dehydrated, the maximum 56.1% furfural yield was obtained over 1 wt% Nb_2O_5 - γ - Al_2O_3 nanofiber, but furfural yield declined to 36.9% when Nb_2O_5 loading reached 33.9 wt%. Those results indicated that the niobia species existed on the γ - Al_2O_3 nanofiber support played the key role on biomass conversion or dehydration.

As shown in Fig. 7, the states of niobia species dispersed on the γ - Al_2O_3 nanofibers can be expressed in such three kinds of structure as a single NbO_6 unit, two-dimensional aggregation and three-dimensional aggregation^{27–30}. If the niobia species exist in the form of a highly dispersed monomer NbO_6 unit, Lewis acid sites are originated from Nb^{6+} ion. At low Nb_2O_5 loading, the niobia species dispersed on the γ - Al_2O_3 nanofiber support through Nb–O–Al bridge bonds. γ - Al_2O_3 has Lewis acid sites with different acid strengths and weak Brønsted acid sites, and the reaction between Nb_2O_5 precursor and hydroxyl groups on the surface of γ - Al_2O_3 nanofiber results in strong metal-support interaction, generating Nb_2O_5 - γ - Al_2O_3 nanofiber with both strong Lewis acid sites and relatively intensive Brønsted acid sites¹⁴. With the increase of Nb_2O_5 loading, the interaction between the isolated niobia species and their nearest neighbors (either isolated or polymerized species) resulted in the formation of Nb–O–Nb bridge bonds. The Brønsted acid sites originated from the Nb–OH–Nb bridge bonds^{27–29}, and the abundance and intensity of Brønsted acid sites could be raised obviously because Nb_2O_5 loading increase could lead to the formation of three-dimensional polymerized niobia species. Nb_2O_5 crystallization caused a rapid decline of the L and B acid sites of Nb_2O_5 - γ - Al_2O_3 nanofiber, which indicated that the crystalline phase Nb_2O_5 has few L and B acid sites³⁰.

It is known that the conversion of glucose to 5-HMF is a two-step reaction. The first step is the isomerization of glucose to fructose catalyzed by Lewis acid and the second step is the dehydration of generated fructose from glucose to 5-HMF under Brønsted acid conditions³¹. Herein, Nb_2O_5 loading increase could lead to the formation of two-dimensional polymerized niobia species, three-dimensional polymerized niobia species and crystallization, which influenced the distribution and quantity of the Lewis acid sites and Brønsted acid sites. On one hand, the Lewis acid site Nb^{6+} play a key role on the isomerization of glucose to fructose, and Brønsted acid sites are more active in the dehydration of generated fructose to 5-HMF^{14,32}. The heterogeneous catalyst with the suitable ratio of Lewis acid sites to Brønsted sites should display an more excellent catalytic performance in the conversion of glucose to 5-HMF in organic solvents³³. Herein, the γ - Al_2O_3 nanofibers loaded with 0.5–1 wt% Nb_2O_5 offers the optimum ratio of Lewis acid sites to Brønsted acid sites, thus they exhibits the best performance in 5-HMF (or furfural) yield from glucose (or xylose) (see Fig. 8). On the other hand, the 1D γ - Al_2O_3 nanofiber support may play an important role on improving 5-HMF yield. For instance, the active Nb_2O_5 catalytic centers are decorated on the external surface of γ - Al_2O_3 fibers, improving the direct interaction between the active sites and glucose. The randomly oriented nanofibers form a large interconnected void (10–20 nm), which made glucose to well contact with the active sites³⁴.

The catalyst re-usability was studied using 1 wt% Nb_2O_5 - γ - Al_2O_3 nanofibers. After reaction, the catalyst was separated from DMSO by centrifugation, and then washed with deionized water and ethanol, dried at 80 °C under vacuum before the next run. From Figs 9 and 10, it is found that the XRD pattern and morphology of catalyst well maintain after one recycle. However, the color of catalyst changed from white to brown, which maybe result from an accumulation of humans on the surface of catalyst¹², which caused some decrease of catalytic performance.

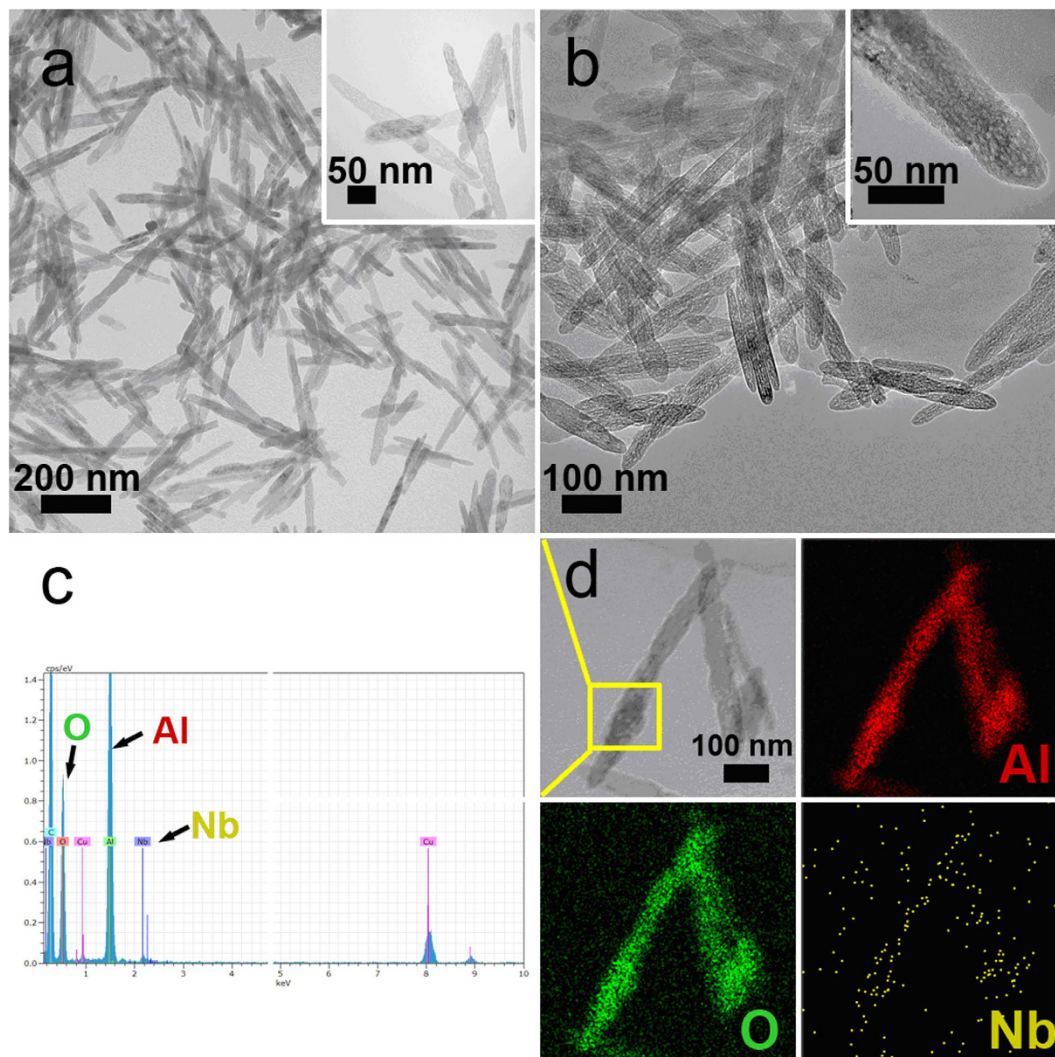


Figure 4. TEM images of γ - Al_2O_3 with different Nb_2O_5 loadings: (a) 0 wt%; (b) 1 wt%. (c) EDX patterns of the selected area of the 1 wt% Nb_2O_5 - γ - Al_2O_3 . (d) The TEM image and elemental mapping of the 1 wt% Nb_2O_5 - γ - Al_2O_3 .

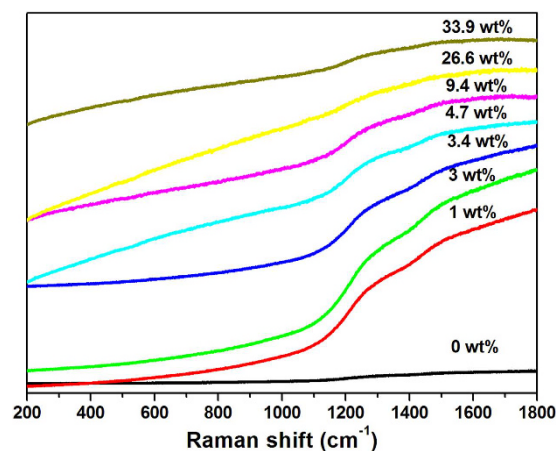


Figure 5. Raman spectra of γ - Al_2O_3 with different Nb_2O_5 loadings.

Conclusions

Nb_2O_5 - γ - Al_2O_3 nanofibers have been prepared by facile incipient-wetness impregnation method to catalyze the conversion of glucose (fructose and xylose as well) into 5-HMF. It is found that $\text{Nb}_2\text{O}_5/\gamma$ - Al_2O_3 nanofibers

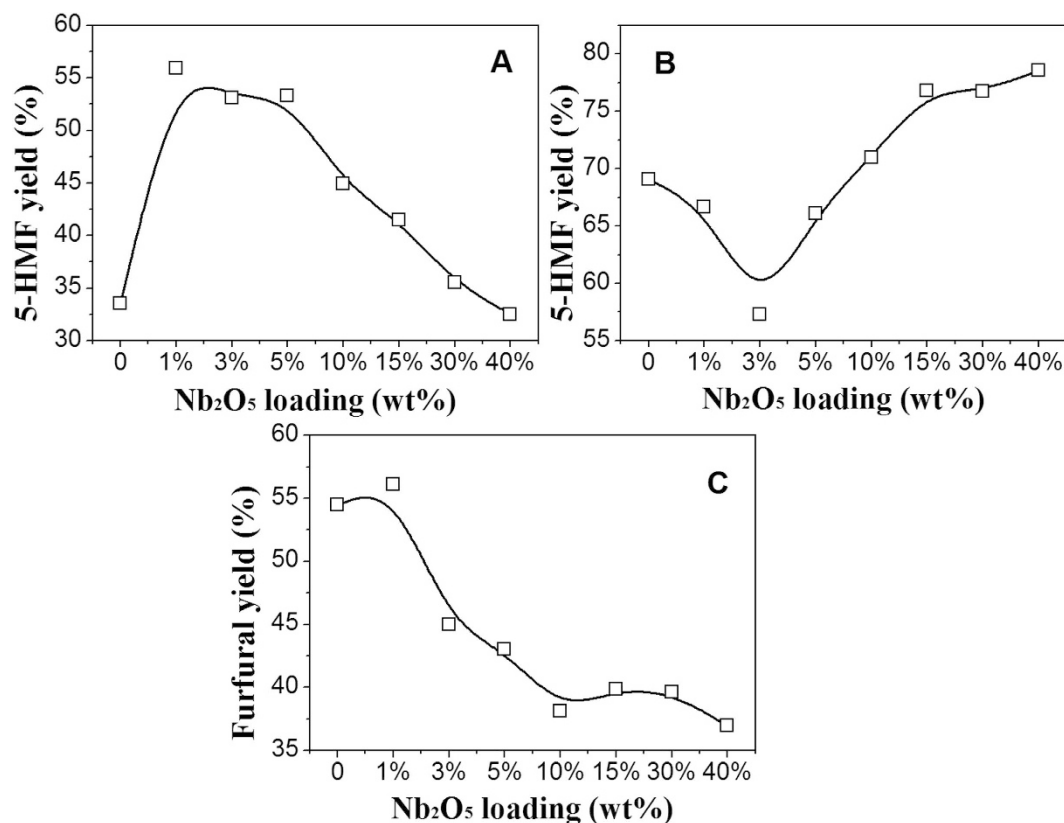


Figure 6. Effect of different Nb₂O₅ loadings on γ -Al₂O₃ on the yield of: 5-HMF from the dehydration of glucose at for 4 hours (A) and fructose for 5 hours (B), furfural from the dehydration of xylose for 6 hours (C) at 150°C.

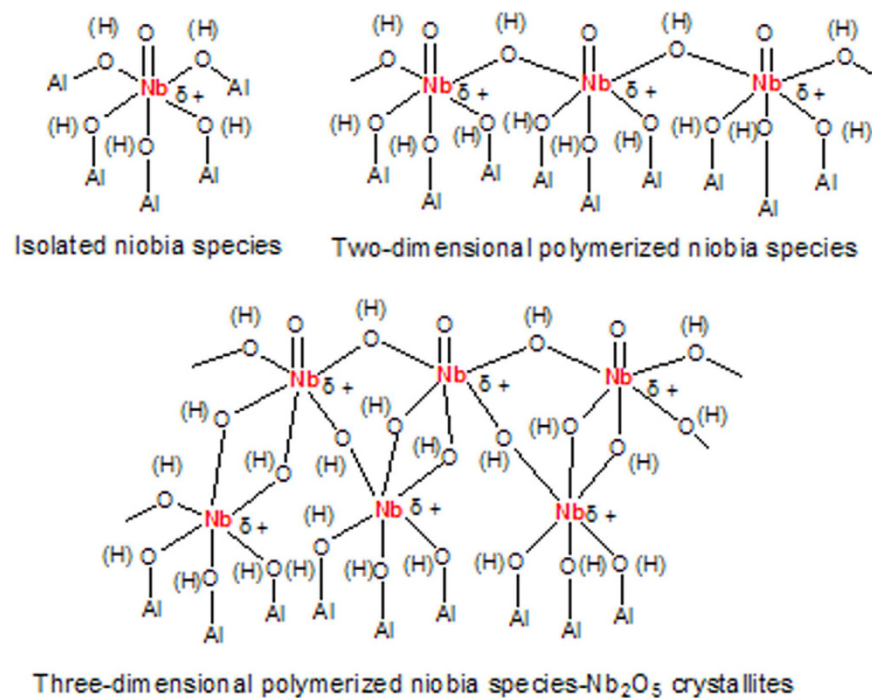


Figure 7. The states of niobia species dispersed on the γ -Al₂O₃ nanofibers.

can efficiently promote the dehydration of glucose, fructose and xylose. The sample with 0.5~1 wt% Nb₂O₅ load exhibits the best performance in glucose conversion into 5-HMF, and 5-HMF yield come up to 55.9~55.9%. This

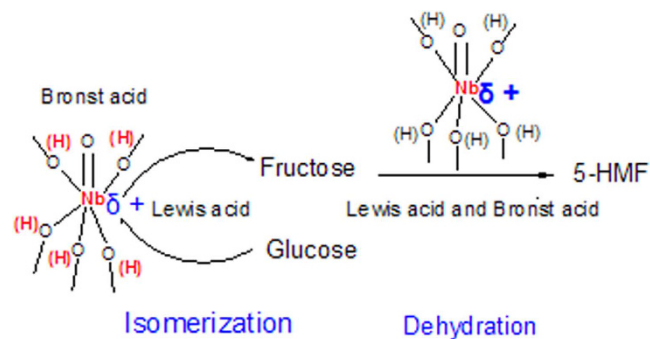


Figure 8. Glucose conversion into 5-HMF over the $\text{Nb}_2\text{O}_5\text{-}\gamma\text{-Al}_2\text{O}_3$.

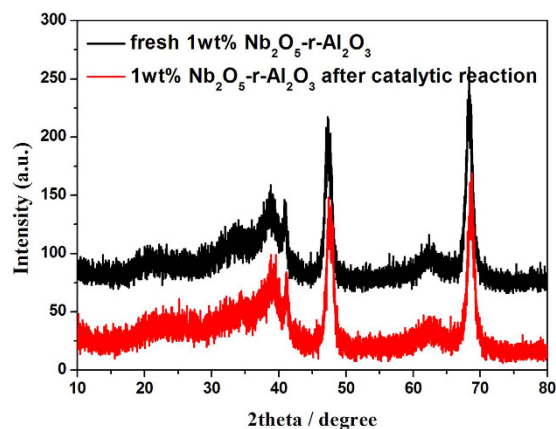


Figure 9. XRD of 1 wt% $\text{Nb}_2\text{O}_5\text{-}\gamma\text{-Al}_2\text{O}_3$ before and after the catalytic reaction.

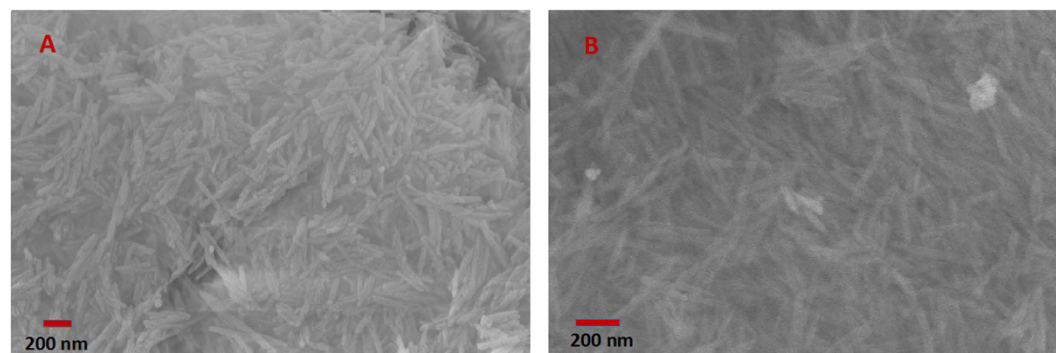


Figure 10. SEM of 1 wt% $\text{Nb}_2\text{O}_5\text{-}\gamma\text{-Al}_2\text{O}_3$ before (A) and after the catalytic reaction (B).

excellent performance of 0.5–1 wt% $\text{Nb}_2\text{O}_5/\gamma\text{-Al}_2\text{O}_3$ nanofibers in glucose conversion into 5-HMF is ascribed to the synergistic effect of suitable ratio of Lewis acid sites to Brønsted acid sites on $\text{Nb}_2\text{O}_5\text{-}\gamma\text{-Al}_2\text{O}_3$ nanofibers.

Methods

Synthesis of supports. All commercially available chemicals and solvents are of reagent grade and were used as received without further purification. The $\gamma\text{-Al}_2\text{O}_3$ nanofibers were prepared by the hydrothermal method. A buffer solution prepared by diluting ammonia (40 mL, 25%) with deionized water to 10%, was used as the precipitation agent. Besides, 30 g $\text{Al}(\text{NO}_3)_3 \cdot 9\text{H}_2\text{O}$ was dissolved in 50 mL deionized water. The buffer solution was loaded into the solution of $\text{Al}(\text{NO}_3)_3$ by dropwise under vigorous stirring until the solution became milky and the initial pH of the mixture ranged from 2.0 to 5.0. The resulting uniform solution was then transferred into a PTFE-lined autoclave and heated in an oven at 200 °C for 48 h. Thereafter, the obtained precipitate was washed several times with deionized water and ethanol by centrifugation, and the obtained precipitate was dried overnight at 55 °C and subsequently calcined in air at 600 °C for 5 h to obtain $\gamma\text{-Al}_2\text{O}_3$ nanofibers.

Preparation of catalysts. $\text{Nb}_2\text{O}_5\text{-}\gamma\text{-Al}_2\text{O}_3$ nanofibers were prepared by the incipient-wetness impregnation method where NbCl_5 was selected as the niobium precursor and incorporated into $\gamma\text{-Al}_2\text{O}_3$ nanofibers. Firstly, the appropriate amount of NbCl_5 was mixed together with the prepared $\gamma\text{-Al}_2\text{O}_3$ nanofibers (0.5 g) in order to obtain catalysts with the controlled Nb_2O_5 loading [wt% = $\text{Nb}_2\text{O}_5/(\text{Nb}_2\text{O}_5 + \text{Al}_2\text{O}_3)$] equal to 1, 3, 5, 10, 15, 30 and 40, respectively. Secondly, the deionized water containing the oxalate with the mole about five times of the mole of NbCl_5 was introduced and then the mixture was kept at room temperature for 48 h. Thirdly, the mixture was dried at 100 °C for 24 h to obtain the different $\text{Nb}_2\text{O}_5\text{-}\gamma\text{-Al}_2\text{O}_3$ catalysts.

Catalytic activity. The glucose, fructose and xylose dehydration reactions were performed in a 15 mL sealed tube (thick walled pressure bottle from Beijing synthware glass) under magnetic stirring. In a typical run, glucose (450 mg), catalyst (45 mg) and DMSO (2.5 ml) were loaded into sealed tube which was then immersed into the preheated oil bath and stirred for a required time. After reaction, the mixture cooled to room temperature naturally, and then the internal standard substances (1-chloronaphthalene) was added into reaction mixture which was further diluted by methanol. The filtered solution was analyzed by HPLC. The dehydration reaction procedures of fructose and xylose were similar to that of glucose, and the glucose (450 mg) was replaced by fructose (450 mg) or xylose (375 mg), respectively.

General Information. The surface morphology and composition of catalysts were characterized by field emission scanning electron microscopy (SEM, JSM-7001F, JEOL, Tokyo, Japan). High-resolution transmission electron microscopy (HRTEM) images were taken on a JEOL JEM-2100F field emission electron microscope under an accelerating voltage of 200 kV equipped with an energy-dispersive X-ray spectroscopy (EDX) instrument (Quantax-STEM, Bruker). The phases structures of catalysts were characterized by powder X-ray diffraction (XRD) analysis using an X-ray diffractometer (DX-2700, China) with Ni-filtered $\text{Cu K}\alpha$ radiation ($\lambda = 1.5406 \text{ \AA}$) at 40 kV and 30 mA with a fixed slit, ranging from 10 to 80°. Surface areas were determined by low temperature N_2 adsorption performed at 77 K, on a 3H-2000PS2 analysis instrument, after pretreatment performed for 8 h at 150 °C under vacuum. The BET (Brunauer-Emmett-Teller) method was used to derive surface areas from the resulting isotherms. Pore size distributions were obtained from analysis of the adsorption branch of the isotherms using Barrette Joynere Halenda (BJH) method. The Raman spectra of these catalysts were determined by Renishaw inVia plus from 200 to 2000 cm^{-1} . The Nb_2O_5 contents of $\text{Nb}_2\text{O}_5\text{-}\gamma\text{-Al}_2\text{O}_3$ nanofibers were characterized by Optima 8000 (ICP-AES). The 5-HMF and furfural were determined by high performance liquid chromatography (HPLC) (L6, China) fitted with a Pgrandasil-TC-C18 column and the ultraviolet detectors for 5-HMF and furfural at 286 nm and 272 nm, respectively. The column oven temperature was set at 25 °C, and the mobile phase was methanol/water = 80:20 (V/V) at a flow rate of 1.0 mL min^{-1} .

References

- van Putten, R. J. *et al.* Hydroxymethylfurfural, A Versatile Platform Chemical Made from Renewable Resources. *Chem. Rev.* **113**, 1499–1597 (2013).
- Zhou, C. H., Xia, X., Lin, C. X., Tong, D. S. & Beltramini, J. Catalytic conversion of lignocellulosic biomass to fine chemicals and fuels. *Chem. Soc. Rev.* **40**, 5588–5617 (2011).
- Ragauskas, A. J. *et al.* The path forward for biofuels and biomaterials. *Science* **311**, 484–489 (2006).
- Xiao, S. H., Liu, B., Wang, Y. M., Fang, Z. F. & Zhang, Z. H. Efficient conversion of cellulose into biofuel precursor 5-hydroxymethylfurfural in dimethyl sulfoxide-ionic liquid mixtures. *Bioresour. Technol.* **151**, 361–366 (2014).
- Li, C. Z., Zhang, Z. H. & Zhao, Z. B. K. Direct conversion of glucose and cellulose to 5-hydroxymethylfurfural in ionic liquid under microwave irradiation. *Tetrahedron Lett.* **50**, 5403–5405 (2009).
- Li, H., Zhang, Q. Y., Bhadury, P. S. & Yang, S. Furan-type Compounds from Carbohydrates via Heterogeneous Catalysis. *Curr. Org. Chem.* **18**, 547–597 (2014).
- Zhang, Y. *et al.* Direct conversion of biomass-derived carbohydrates to 5-hydroxymethylfurfural over water-tolerant niobium-based catalysts. *Fuel* **139**, 301–307 (2015).
- Jimenez-Morales, I., Moreno-Recio, M., Santamaria-Gonzalez, J., Maireles-Torres, P. & Jimenez-Lopez, A. Production of 5-hydroxymethylfurfural from glucose using aluminium doped MCM-41 silica as acid catalyst. *Appl. Catal. B: Environ.* **164**, 70–76 (2015).
- Jain, A., Shore, A. M., Jonnalagadda, S. C., Ramanujachary, K. V. & Mugweru, A. Conversion of fructose, glucose and sucrose to 5-hydroxymethyl-2-furfural over mesoporous zirconium phosphate catalyst. *Appl. Catal. A Gen.* **489**, 72–76 (2015).
- Combs, E., Cinlar, B., Pagan-Torres, Y., Dumesic, J. A. & Shanks, B. H. Influence of alkali and alkaline earth metal salts on glucose conversion to 5-hydroxymethylfurfural in an aqueous system. *Catal. Commun.* **30**, 1–4 (2013).
- Yang, Y., Hu, C. W. & Abu-Omar, M. M. The effect of hydrochloric acid on the conversion of glucose to 5-hydroxymethylfurfural in $\text{AlCl}_3\text{-H}_2\text{O/THF}$ biphasic medium. *J. Mol. Catal. A Chem.* **376**, 98–102 (2013).
- Kuo, C. H. *et al.* Heterogeneous acidic TiO_2 nanoparticles for efficient conversion of biomass derived carbohydrate. *Green Chem.* **16**, 785–791 (2014).
- Yang, F. L., Liu, Q. S., Yue, M., Bai, X. F. & Du, Y. G. Tantalum compounds as heterogeneous catalysts for saccharide dehydration to 5-hydroxymethylfurfural. *Chem. Commun.* **47**, 4469–4471 (2011).
- Wang, H., Yao, Z. Y., Zhan, X. C., Wu, Y. & Li, M. Preparation of highly dispersed $\text{W/ZrO}_2\text{-Al}_2\text{O}_3$ hydrodesulfurization catalysts at high WO_3 loading via a microwave hydrothermal method. *Fuel* **158**, 918–926 (2015).
- Stosic, D., Bennici, S., Pavlovic, V., Rakic, V. & Auroux, A. Tuning the acidity of niobia: Characterization and catalytic activity of $\text{Nb}_2\text{O}_5\text{-MeO}_2$ (Me = Ti, Zr, Ce) mesoporous mixed oxides. *Mater. Chem. Phys.* **146**, 337–345 (2014).
- Xia, Y. N. *et al.* One-dimensional nanostructures: Synthesis, characterization, and applications. *Adv. Mater.* **15**, 353–389 (2003).
- Shen, S. C. *et al.* Steam-assisted solid wet-gel synthesis of high-quality nanorods of boehmite and alumina. *J. Phys. Chem. C* **111**, 700–707 (2007).
- Wang, F., Wu, H. Z., Liu, C. L., Yang, R. Z. & Dong, W. S. Catalytic dehydration of fructose to 5-hydroxymethylfurfural over Nb_2O_5 catalyst in organic solvent. *Carbohydr. Res.* **368**, 78–83 (2013).
- Brunauer, S., Deming, L. S., Deming, W. E. & Teller, E. Chemisorptions of Gases on Iron Synthetic Ammonia Catalysts. *J. Am. Chem. Soc.* **62**, 1723–1732 (1940).
- Liu, J. *et al.* Catalytic conversion of glucose to 5-hydroxymethylfurfural over nano-sized mesoporous $\text{Al}_2\text{O}_3\text{-B}_2\text{O}_3$ solid acids. *Catal. Commun.* **62**, 19–23 (2015).

21. Zhu, H. Y. *et al.* Manipulating the size and morphology of aluminum hydrous oxide nanoparticles by soft-chemistry approaches. *Microporous Mesoporous Mater.* **85**, 226–233 (2005).
22. Jiao, W. Q., Wang, Y. M. & He, M. Y. Morphology-controlled synthesis of gamma-Al₂O₃ with large mesopores through combustion of aluminum carboxylate salts. *Microporous Mesoporous Mater.* **181**, 123–131 (2013).
23. Wachs, I. E. Raman and IR studies of surface metal oxide species on oxide supports: Supported metal oxide catalysts. *Catal. Today.* **27**, 437–455 (1996).
24. Kitano, T. *et al.* Acid property of Nb₂O₅/Al₂O₃ prepared by impregnation method by using niobium oxalate solution: Effect of pH on the structure and acid property. *Catal. Today.* **226**, 97–102 (2014).
25. Dutta, S. *et al.* Microwave assisted rapid conversion of carbohydrates into 5-hydroxymethylfurfural catalyzed by mesoporous TiO₂ nanoparticles. *Appl. Catal. A Gen.* **409**, 133–139 (2011).
26. Yi, X. H. *et al.* A heteropoly acid ionic crystal containing Cr as an active catalyst for dehydration of monosaccharides to produce 5-HMF in water. *Catal. Sci. Technol.* **5**, 2496–2502 (2015).
27. He, J. & Fan, Y. N. Dispersion States and Bronsted Acidity Feature of Nb(2)O(5) on t-ZrO₂. *Acta Phys. Chim. Sin.* **27**, 2416–2420 (2011).
28. Sun, C. Z. *et al.* Dispersion, reduction and catalytic performance of CuO supported on ZrO₂-doped TiO₂ for NO removal by CO. *Appl. Catal. B* **103**, 206–220 (2011).
29. Jehng, J. M., Turek, A. M. & Wachs, I. E. Surface modified niobium oxide catalyst: synthesis, characterization, and catalysis. *Appl. Catal. A* **83**, 179–200 (1992).
30. Tanabe, K. Niobic acid as an unusual acidic solid material. *Mater. Chem. Phys.* **17**, 217–225 (1987).
31. Atanda, L., Mukundan, S., Shrotri, A., Ma, Q. & Beltramini, J. Catalytic Conversion of Glucose to 5-Hydroxymethyl-furfural with a Phosphated TiO₂ Catalyst. *Chem Cat Chem* **7**, 781–790 (2015).
32. Sun, M. Y., Nicosia, D. & Prins, R. The effects of fluorine, phosphate and chelating agents on hydrotreating catalysts and catalysis. *Catal. Today* **86**, 173–189 (2003).
33. Wang, J. J. *et al.* Direct conversion of carbohydrates to 5-hydroxymethylfurfural using Sn-Mont catalyst. *Green Chem.* **14**, 2506–2512 (2012).
34. Yang, D. J. *et al.* Alumina nanofibers grafted with functional groups: A new design in efficient sorbents for removal of toxic contaminants from water. *Water Res.* **44**, 741–750 (2010).

Acknowledgements

This work is financially supported by the National Natural Science Foundation of China (Nos 21207073, 51473081 and 21376177), ARC Discovery Project (Grant No. 130104759), and State Key Lab of Multiphase Flow in Power Engineering for financial support.

Author Contributions

The experiment and characterization work is done by H.J., X.Z., C.L. and Y.W. D.Y., Z.L. and X.Y. wrote the main manuscript text and prepared figures All authors reviewed the manuscript.

Additional Information

Competing financial interests: The authors declare no competing financial interests.

How to cite this article: Jiao, H. *et al.* Nb₂O₅-γ-Al₂O₃ nanofibers as heterogeneous catalysts for efficient conversion of glucose to 5-hydroxymethylfurfural. *Sci. Rep.* **6**, 34068; doi: 10.1038/srep34068 (2016).



This work is licensed under a Creative Commons Attribution 4.0 International License. The images or other third party material in this article are included in the article's Creative Commons license, unless indicated otherwise in the credit line; if the material is not included under the Creative Commons license, users will need to obtain permission from the license holder to reproduce the material. To view a copy of this license, visit <http://creativecommons.org/licenses/by/4.0/>

© The Author(s) 2016